

## Anti-HIV-1 activity of 3-deaza-adenosine analogs Inhibition of *S*-adenosylhomocysteine hydrolase and nucleotide congeners

Richard K. Gordon<sup>1</sup>, Krzysztof Ginalski<sup>2</sup>, Witold R. Rudnicki<sup>3</sup>, Leszek Rychlewski<sup>4</sup>, Marvin C. Pankaskie<sup>5</sup>, Janusz M. Bujnicki<sup>6</sup> and Peter K. Chiang<sup>1</sup>

<sup>1</sup>Walter Reed Army Institute of Research, Washington, USA; <sup>2</sup>University of Texas, Southwestern Medical Center, Dallas, USA; <sup>3</sup>Interdisciplinary Centre for Mathematical and Computational Modelling, Warsaw University, Poland; <sup>4</sup>BioInfoBank Institute, Poznań, Poland; <sup>5</sup>School of Pharmacy, Palm Beach Atlantic University, West Palm Beach, Florida, USA; <sup>6</sup>Bioinformatics Laboratory, International Institute of Molecular and Cell Biology, Warsaw, Poland

Eight adenosine analogs, 3-deaza-adenosine (DZA), 3-deaza-(±)aristeromycin (DZAri), 2',3'-dideoxy-adenosine (ddAdo), 2',3'-dideoxy-3-deaza-adenosine (ddDZA), 2',3'-dideoxy-3-deaza-(±)aristeromycin (ddDZAri), 3-deaza-5'-(±)noraristeromycin (DZNAri), 3-deaza-neplanocin A (DZNep), and neplanocin A (NepA), were tested as inhibitors of human placenta *S*-adenosylhomocysteine (AdoHcy) hydrolase. The order of potency for the inhibition of human placental AdoHcy hydrolase was: DZNep ≈ NepA ≫ DZAri ≈ DZNAri > DZA ≫ ddAdo ≈ ddDZA ≈ ddDZAri. These same analogs were examined for their anti-HIV-1 activities measured by the reduction in p24 antigen produced by 3'-azido-3'-deoxythymidine (AZT)-sensitive HIV-1 isolates, A012 and A018, in phytohemagglutinin-stimulated peripheral blood mononuclear (PBMCs) cells. Interestingly, DZNAri and the 2',3'-dideoxy 3-deaza-nucleosides (ddAdo, ddDZAri, and ddDZA) were only marginal inhibitors of p24 antigen production in HIV-1 infected PBMC. DZNAri is unique because it is the only

DZA analog with a deleted methylene group that precludes anabolic phosphorylation. In contrast, the other analogs were potent inhibitors of p24 antigen production by both HIV-1 isolates. Thus it was postulated that these nucleoside analogs could exert their antiviral effect via a combination of anabolically generated nucleotides (with the exception of DZNAri), which could inhibit reverse transcriptase or other viral enzymes, and the inhibition of viral or cellular methylation reactions. Additionally, QSAR-like models based on the molecular mechanics (MM) were developed to predict the order of potency of eight adenosine analogs for the inhibition of human AdoHcy hydrolase. In view of the potent antiviral activities of the DZA analogs, this approach provides a promising tool for designing and screening of more potent AdoHcy hydrolase inhibitors and antiviral agents.

**Keywords:** HIV-1; 3-deaza-adenosine; *S*-adenosylhomocysteine hydrolase inhibitors; antiviral agents; modeling.

Correspondence to K. Ginalski, Department of Biochemistry, University of Texas, Southwestern Medical Center, 5323 Harry Hines Blvd., Dallas, TX 75390, USA.

Fax: + 1 214 648 9099, Tel.: + 1 214 648 6363,

E-mail: kinal@chop.swmed.edu or

P. K. Chiang, Division of Experimental Therapeutics, Walter Reed Army Institute of Research, Silver Spring, MD 20910-7500, USA.

Fax: + 1 301 319 9449, Tel.: + 1 301 319 9849,

E-mail: peter.chiang@na.amedd.army.mil or

R. K. Gordon, Walter Reed Army Institute of Research, Silver Spring, MD 20910-7500, USA. Tel.: + 1 301 319 9987,

E-mail: richard.gordon@na.amedd.army.mil

**Abbreviations:** AdoHcy, *S*-adenosylhomocysteine; AdoMet, *S*-adenosylmethionine; DZA, 3-deaza-adenosine; DZAri, 3-deaza-(±)-aristeromycin; ddAdo, 2',3'-dideoxy-adenosine; ddDZA, 2',3'-dideoxy-3-deaza-adenosine; ddDZAri, 2',3'-dideoxy-3-deaza-(±)-aristeromycin; DZNAri, 3-deaza-5'-(±)noraristeromycin; DZNep, 3-deaza-neplanocin A; NepA, neplanocin A; AZT, 3'-azido-3'-deoxythymidine; PBMC, peripheral blood mononuclear cells; NAD, nicotinamide adenine dinucleotide; AK, adenosine kinase; dCK, deoxycytidine kinase; TK, thymidine kinase; TCID<sub>50</sub>, 50% tissue culture infectious dose.

**Enzyme:** *S*-adenosylhomocysteine hydrolase (EC 3.3.1.1).

(Received 26 May 2003, accepted 25 June 2003)

The 3-deaza-nucleoside analogs of adenosine (Fig. 1), 3-deaza-adenosine (DZA), 3-deaza-(±)aristeromycin (DZAri), and 3-deaza-neplanocin A (DZNep) are potent inhibitors of *S*-adenosylhomocysteine hydrolase (AdoHcy hydrolase) [1,2]. These analogs can exert a variety of biological effects including remarkable antiviral activities [3–6]. Inhibition of AdoHcy hydrolase results in the inhibition of *S*-adenosylmethionine (AdoMet)-dependent methylation reactions, including DNA, RNA, protein, and lipid methylation. Evidence supporting the potential inhibition of AdoMet-dependent methylation reactions in the antiviral activity of the DZA analogs include correlations of viral reduction with AdoHcy hydrolase inhibition, markedly elevated levels of AdoHcy and to a lesser extent AdoMet, and the formation of nucleoside congeners, e.g. 3-deaza-adenosylhomocysteine or 3-deaza-adenosylmethionine from DZA. Therefore, a methylation hypothesis for the antiviral activity encompasses the blocking of AdoHcy hydrolase by the inhibitors, giving rise to the intracellular level of AdoHcy, and by feedback inhibition decreases AdoMet-dependent methylation reactions within cells. It is this mode of action that is attributed to the suppression in virus replication and/or viral methylation-dependent processes [1,7].

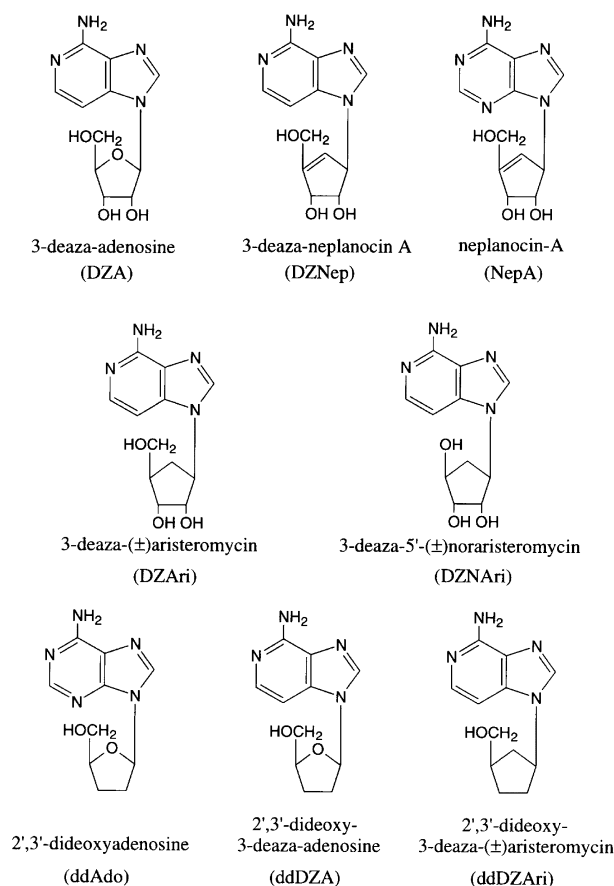


Fig. 1. Chemical structures of the nucleosides used in this study.

An alternative, but not mutually exclusive, antiviral mechanism for the DZA analogs is their anabolism to their mono-, di-, and tri-phosphate forms [8,9]. Nucleoside anti-HIV-1 agents such as 3'-azido-3'-deoxythymidine (AZT) have a common mode of action. First, the nucleoside agents are metabolically converted to their triphosphate nucleotide analogs, which then selectively inhibit viral nucleic acid polymerase. The current hypothesis is that AZT-triphosphate competes with deoxythymidine 5'-triphosphate for the viral reverse transcriptase, and, additionally, AZT-triphosphate acts as a chain terminator after incorporation into the nascent 3'-terminus.

Recently, we demonstrated that the DZA analogs caused a marked reduction in p24 antigen production in the phytohemagglutinin (PHA)-stimulated human peripheral blood mononuclear cells (PBMC) and H9 cells infected with HIV-1. Also, the 3-deaza-nucleosides might undergo intracellular phosphorylation to be metabolized to their respective triphosphate nucleotides in diverse cell types [10–12]. However, the anabolic pathway(s) involved in the conversion has not been completely elucidated [11,13,14]. This missing information precludes the enzymatic synthesis of the 3-deaza-nucleotide analogs for a direct examination of its effect on HIV-1 enzymes. Furthermore, a chemical synthetic route needs to be elucidated.

Traditionally, the biological effects of the DZA analogs have been attributed to their potent inhibition of AdoHcy

hydrolase and the attendant inhibition of methylation reactions [1,7,15,16]. However, the antiviral mechanism of the DZA analogs remains unclear, i.e. whether it is due to the inhibition of methylation, perturbation of viral enzymes by 3-deaza-nucleotides, or a combination of both. To preclude the cellular phosphorylation of the DZA analogs to their nucleotides, 5'-(±)noraristeromycin and 3-deaza-5'-(±)noraristeromycin (DZNAri) were synthesized [17,18]. These compounds lack the phosphate accepting 5'-hydroxyl moiety because it has been modified to a secondary hydroxyl by the removal of a methylene group (Fig. 1). Both compounds were found to have poor antiviral activity. In contrast, both noraristeromycin and DZNAri exhibited only a small reduction in their inhibition of AdoHcy hydrolase derived from mouse L929 cells. These results suggest that AdoHcy hydrolase and cellular methylation processes may not be the only pharmacological targets of the 3-deaza-nucleosides as expressed by their inhibition of HIV-1 [10]. Thus, the 3-deaza-nucleosides may be anabolically converted to their respective 3-deaza-nucleotides, which would then inhibit the HIV-1 reverse transcriptase.

The present study was undertaken to elucidate the contribution of these two mechanisms: (a) indirect inhibition of methylation via the direct inhibition of AdoHcy hydrolase, and (b) intracellular phosphorylation of the DZA analogs to become inhibitors of HIV-1 production similar to the effect of AZT. Thus, the potency of the DZA analogs (Fig. 1) to reduce HIV-1 p24 antigen production was compared with the inhibition of human AdoHcy hydrolase. In addition, simple QSAR-like theoretical methodologies were developed for predicting the binding energies of the DZA analogs to AdoHcy hydrolase. These models overcome the limitations of more sophisticated approaches for calculating the exact binding free energy, which are computationally very intensive and limited in practical applications. These molecular mechanics (MM)-based models are ideal for the fast and effective screening of new adenosine derivatives that are potential inhibitors of AdoHcy hydrolase.

Recently, after these modeling studies had been completed, the experimental crystal structure of AdoHcy hydrolase complexed with NepA and NAD molecules was reported [19]. This enabled verification of our proposed 3D model for this ligand–protein complex and provided a very useful test for validation of the applied theoretical methods and modeling strategy.

## Materials and methods

### Chemical synthesis of 3-deaza-adenosine analogs

2',3'-Dideoxy-adenosine (ddAdo), 2',3'-dideoxy-3-deaza-adenosine (ddDZA), and 2',3'-dideoxy-3-deaza-(±)aristeromycin were prepared from adenosine, DZA, and DZAri, respectively, by reacting the nucleoside with 2-acetoxyisobutanol bromide followed by catalytic reduction of the resulting olefin and recrystallization of the final product from methanol or ethanol [16,20,21]. 3-Deaza-5'-(±)noraristeromycin was prepared according to the method of Siddiqi [18]. All compounds were characterized by NMR, mass spectra, and elemental analysis.

### AdoHcy hydrolase assay

Human placental AdoHcy hydrolase was a kind gift from Michael S. Hershfield (Duke University Medical Center, Durham, NC 27710) and was purified as described and stored at  $-80^{\circ}\text{C}$  [22]. Assay conditions for the hydrolase followed previously described methods [23]. Prior to use, the  $[8-^{14}\text{C}]$ adenosine ( $43.2\text{ mCi}\cdot\text{mmol}^{-1}$ ) was checked for purity using isocratic HPLC elution ( $\text{C}_{18}$   $\mu$ BondaPak column from Waters Associates, Milford, MA, USA, 60 mM triethylammonium acetate, adjusted to pH 4 with acetic acid). The assay incubation mixture contained 0.4 IU of enzyme in 50  $\mu\text{L}$ . The metabolites were separated by thin-layer chromatography (cellulose with fluorescent indicator: 2-propanol/concentrated ammonia/water, 7 : 1 : 2, v/v/v). The radioactivity was quantitated by cutting the plastic backed TLC plates and placing them in scintillation vials, and counting in a Packard 2000 CA scintillation counter (Packard Instruments, Chicago, IL, USA).

### Inhibition of HIV-1 p24 antigen production in PBMCs

The HIV-1 strains used, A012 and A018, were obtained from National Institutes of Health AIDS Research and Reagent Reference Program. Inhibition of p24 antigen was measured as described previously [10,24]. Briefly, PHA-stimulated PBMCs were incubated with either HIV-1 strain for 1 h at  $37^{\circ}\text{C}$  at 200-fold the 50% tissue culture infectious dose ( $\text{TCID}_{50}$ ) of the virus stock per  $2 \times 10^5$  PBMC cells. The  $\text{TCID}_{50}$  was defined as the amount of virus stock at which 50% of the inoculated wells were positive. Cells were then grown in microtiter plates with different drug concentrations at  $2 \times 10^5$  cells per well. On day 4, cells were resuspended and split 1 : 3 with fresh media and drugs. Supernatant p24 antigen was determined on day 7 by ELISA (Coulter). The views and opinions expressed herein are those of the authors and do not reflect the official position of the US Army or the Department of Defense. Guidelines for human experimentation of the US Department of Defense were followed in the conduct of the clinical research. Informed consent was obtained in writing from each subject.

### Cell lines

H9 cells (American Type Culture Collection, Manassas, VA, USA), an HIV-1 permissive human T-cell lymphoma, were grown in suspension with RPMI 1640 supplemented with 20% fetal bovine serum, 2 mM L-glutamine, 100  $\text{U}\cdot\text{mL}^{-1}$  penicillin, and 100  $\mu\text{g}\cdot\text{mL}^{-1}$  streptomycin, and 5%  $\text{CO}_2$  at  $36^{\circ}\text{C}$ . AA-2 cells ( $\text{AK}^-$ ,  $\text{dCK}^-$ ), which lack adenosine kinase and deoxycytidine kinase, were obtained through the AIDS Research and Reference Reagent Program, NIH, and grown in suspension in H9 media containing 10% fetal bovine serum [25] V79 lung fibroblasts containing thymidine kinase V79 ( $\text{TK}^+$ ) or lacking thymidine kinase V79 ( $\text{TK}^-$ ) were provided by J. Nyce (East Carolina University, Greenville, NC, USA) and grown in DMEM with the same additions as the AA-2 cells [26]. The  $\text{AK}^-$ ,  $\text{dCK}^-$ , and  $\text{TK}^-$  cells yielded background values for the expression of the respective enzymes they were lacking (data not shown).

### AdoMet and AdoHcy metabolites

Approximately  $2 \times 10^8$  H9 cells were incubated with 200  $\mu\text{Ci}$   $[^{35}\text{S}]$ methionine for 60 min. The cells were resuspended with appropriate drugs for up to 3 h. The reaction was terminated by centrifuging the cells (1000 g, 5 min,  $4^{\circ}\text{C}$ ), and then adding cold 5% trichloroacetic acid. Samples were sonicated for 15 s on ice. After neutralizing with  $\text{Na}_2\text{CO}_3$  and concentrating the supernatant by lyophilization [12], AdoMet and AdoHcy levels were determined by HPLC using a  $\text{C}_{18}$  column (Waters Associates) and in-line radioactive detection as previously described [10,27]. The elution times for AdoMet and AdoHcy were  $\approx 7$  and  $\approx 29$  min, respectively.

### Nucleotides of DZNep and DZAri

H9, AA-2, and the two V79 cloned cells in log phase were incubated with 1  $\mu\text{M}$   $[^3\text{H}]\text{DZAri}$  ( $14\text{ Ci}\cdot\text{mmol}^{-1}$ ) or  $[^3\text{H}]\text{DZNep}$  ( $1.6\text{ Ci}\cdot\text{mmol}^{-1}$ ) (Moravek Biochemicals, Brea, CA) at about  $1 \times 10^6$  cells $\cdot\text{mL}^{-1}$  for 18 h. As previously described [10], the cells were washed, sonicated for 15 s on ice, and the extracted nucleotides were analyzed by HPLC with a Whatman Partisil 10 SAX anion exchange column (Whatman, Hillsboro, OR, USA). The initial buffer was 5 mM  $\text{NH}_4\text{H}_2\text{PO}_4$  (pH 2.8), followed by a linear gradient over 50 min to 750 mM  $\text{NH}_4\text{H}_2\text{PO}_4$  (pH 3.5) at a flow of 1.5  $\text{mL}\cdot\text{min}^{-1}$ . Radioactive peaks of the 3-deaza-nucleotides were monitored with a Flo-One\Beta with 4  $\text{mL}\cdot\text{min}^{-1}$  of Flo-Scint III scintillator (Packard Instruments, Chicago, IL, USA). The identification of the triphosphates was based on retention times obtained previously and by hydrolysis to the parent compound [10,12]:  $[^3\text{H}]\text{DZAri}$ -triphosphate,  $\approx 38$  min;  $[^3\text{H}]\text{DZNep}$ -triphosphate,  $\approx 39$  min.

### 3D models of AdoHcy hydrolase–adenosine analogs complexes

Assuming that strongly related ligands have similar binding modes, 3D models for the inhibitor-NAD-AdoHcy hydrolase complexes were built based on available crystallographic structures of this protein complexed with 2'-hydroxy,3'-ketocyclopent-4'-enyladenine [28] and adenosine [29] by using the INSIGHTII program package (Accelrys Inc., San Diego, CA, USA). The coordinates for human AdoHcy hydrolase and NAD (nicotinamide adenine dinucleotide) were derived from PDB accession no. 1A7A [28]. Adenosine analogs were modeled based on 2'-hydroxy, 3'-ketocyclopent-4'-enyladenine for DZNep and NepA, and adenosine for DZA, DZAri, DZNAri, ddAdo, ddDZA, and ddDZAri using superimposed human (PDB accession no. 1A7A) and rat (PDB accession no. 1D4F) AdoHcy hydrolase C $\alpha$  atoms [29].

### MM-based minimization of 3D models

All models were subjected to a series of energy optimizations with the DISCOVER module of INSIGHTII until the r.m.s. gradient was smaller than  $0.1\text{ kcal}\cdot\text{mol}^{-1}\cdot\text{\AA}^{-2}$ . All energy optimizations were performed in a CFF97 forcefield [30,31] with a distance-dependent dielectric constant of  $4r$ , using the steepest descent and conjugate gradient methods. Partial charges for all the ligand molecules were calculated by the

charge equilibration method [32] implemented in CERIU2 (Accelrys Inc.). Main-chain atoms of the protein as well as the heavy atoms of NAD were restrained by harmonic forces and a force constant of  $100 \text{ kcal}\cdot\text{mol}^{-1}\cdot\text{\AA}^{-2}$ . To avoid uncontrolled global conformational changes of the protein, optimizations were performed only for the active center region. All atoms in residues further from the active center than 10 Å were fixed. The energy of the complex ( $E_{\text{complex}}^{\text{min}}$ ) was obtained as the final energy after optimization of the system. Protein and ligand structures were extracted separately from the minimized complex, and their respective energies ( $E_{\text{protein}}^{\text{min}}$ ) and ( $E_{\text{inhibitor}}^{\text{min}}$ ), were computed without further minimization.

### Calculation of binding energies

In this study a simple, QSAR-like approach, based on the molecular mechanics is used. The binding constants for a set of ligands are correlated with the binding energies obtained from the constrained energy minimization. This approach is related to the linear interaction energy model introduced by Aqvist [33,34]. In the original linear interaction energy model, binding energies are computed using time-averaged electrostatic and van der Waals components of the total energy obtained during molecular dynamics simulation of the system in bound and nonbound state. In our approach, time-averages of the component energies are replaced by the energy of the optimal conformation of the complex in the bound and nonbound state, respectively. This approach is not universal, but in the case, where ligand binds in single, well defined conformation in a tight binding pocket, it could be expected that time average of the system energy is connected with the minimum energy by the following relation:

$$\langle E \rangle = E_{\text{min}} + \frac{Nk_{\text{B}}T}{2} \quad (1)$$

where  $N$  is a number of degrees of freedom,  $k_{\text{B}}$  is the Boltzmann constant and  $T$  is temperature in Kelvin. Therefore, after simple calculations it can be shown that energy of the interaction is given by:

$$\langle E_{\text{INT}} \rangle = E_{\text{complex}}^{\text{min}} + \frac{N_{\text{complex}}k_{\text{B}}T}{2} - E_{\text{protein}}^{\text{min}} - \frac{N_{\text{protein}}k_{\text{B}}T}{2} - E_{\text{ligand}}^{\text{min}} - \frac{N_{\text{ligand}}k_{\text{B}}T}{2} \quad (2)$$

and as  $N_{\text{complex}} = N_{\text{protein}} + N_{\text{ligand}}$ ,

$$\langle E_{\text{INT}} \rangle = \Delta E = E_{\text{complex}}^{\text{min}} - E_{\text{protein}}^{\text{min}} - E_{\text{ligand}}^{\text{min}} \quad (3)$$

In contrast to the original linear interaction energy model, in this study solvent molecules were not explicitly included in the system. Therefore no coefficients relating interaction energy and the free energy of binding were used. Instead linear, QSAR-like models based on correlation between free energy of binding and interaction energy were proposed. In contrast to QSAR, there are no fitted parameters and it is assumed that all contributions to the free energy of binding are correlated with the direct interaction energy between protein and ligand.

Two models were used to compute the energy of binding of 3-deaza-adenosine analogs in the active site of AdoHcy

hydrolase, which differed with their treatment of the solvent effects. In the basic model, which completely neglects the solvent effects, the binding energy was calculated using the formula:

$$\Delta E = E_{\text{complex}}^{\text{min}} - E_{\text{protein}}^{\text{min}} - E_{\text{inhibitor}}^{\text{min}} \quad (4)$$

The term corresponding to the protein energy was an average for all structures obtained with various ligands. This approach has been successfully used to predict strength of binding between anthracycline antibiotics and DNA [35], nevertheless, binding energies predicted by this model are unphysical (unrealistically large). In the extended model, the solvent effects were accounted for in an averaged manner by introducing a term proportional to the surface area (A):

$$E^{\text{surface}} = k_{\text{s}}A \quad (5)$$

where  $E^{\text{surface}}$  is an energy term proportional to the surface and  $k_{\text{s}}$  is a proportionality constant. The program NACCESS was used to compute the solvent accessible surface area for the complex of protein and inhibitor [36]. The resulting surface energy term was added to the total energy. Thus, the binding energy was modified in the following way:

$$\Delta E = E_{\text{complex}}^{\text{min}} - E_{\text{protein}}^{\text{min}} - E_{\text{inhibitor}}^{\text{min}} + E_{\text{complex}}^{\text{surface}} - E_{\text{protein}}^{\text{surface}} - E_{\text{inhibitor}}^{\text{surface}} \quad (6)$$

The coefficient  $k_{\text{s}}$  was chosen to reduce binding energies to a more realistic range. In both models, the total energy of a protein molecule was assigned either as the energy of a protein in complex with a given compound or as an averaged energy obtained for all the compounds. The averaged protein energy was introduced to reflect the conformational freedom of the protein in the apo state.

## Results

### Inhibition of human AdoHcy hydrolase by the DZA analogs

Among all the DZA analogs tested (Table 1), NepA was the most potent inhibitor of the human placental AdoHcy

**Table 1.** IC<sub>50</sub> values for the inhibition of p24 antigen in PBMC infected with HIV-1 isolates and K<sub>i</sub> values for the inhibition of human placental S-adenosylhomocysteine hydrolase. Replicates were  $n \geq 2$  for IC<sub>50</sub> and  $n \geq 3$  for K<sub>i</sub> values. All values are shown as mean  $\pm$  SD.

Compound	IC <sub>50</sub> (μM)		K <sub>i</sub> (μM) AdoHcy hydrolase
	A012 isolate	A018 isolate	
NepA	0.011 $\pm$ 0.005 <sup>a</sup>	0.018 $\pm$ 0.009 <sup>a</sup>	0.007 $\pm$ 0.002
DZNep	0.010 $\pm$ 0.001 <sup>a</sup>	0.016 $\pm$ 0.005 <sup>a</sup>	0.023 $\pm$ 0.008
DZAri	0.14 $\pm$ 0.06 <sup>a</sup>	0.22 $\pm$ 0.02 <sup>a</sup>	0.24 $\pm$ 0.04
DZNAri	3.48 $\pm$ 0.3	2.84 $\pm$ 0.3	0.83 $\pm$ 0.15
DZA	0.15 $\pm$ 0.06 <sup>a</sup>	0.20 $\pm$ 0.02 <sup>a</sup>	3.9 $\pm$ 0.7
ddAdo	6.3 $\pm$ 0.4	4.8 $\pm$ 0.2	28.0 $\pm$ 4.1
ddDZA	4.8 $\pm$ 0.3	2.5 $\pm$ 0.3	30.1 $\pm$ 3.0
ddDZAri	3.7 $\pm$ 0.3	2.0 $\pm$ 0.2	50.5 $\pm$ 7.3

<sup>a</sup> The IC<sub>50</sub> values from Mayers *et al.* [10].

hydrolase with a  $K_i$  of 0.007  $\mu\text{M}$ . Next in potency was DZNep, yielding a  $K_i$  of 0.023  $\mu\text{M}$ ,  $\approx$  threefold less potent than NepA. Whereas DZAri showed a  $K_i$  of 0.24  $\mu\text{M}$ , its congener DZNari was  $\approx$  threefold less potent, with a  $K_i$  of 0.83  $\mu\text{M}$ . DZA itself was almost fivefold less potent than DZNari. The least potent inhibitors were the dideoxy analogs, and as a group were at least 10-fold less potent than DZA.

### Inhibition of AdoHcy hydrolase: effect on the AdoMet/AdoHcy ratio

In H9 cells prelabelled with [ $^{35}\text{S}$ ]methionine, significant elevations in AdoHcy levels were observed after treatment with 100  $\mu\text{M}$  DZNari or 1  $\mu\text{M}$  DZNep over 3 h (Fig. 2, top). Note that DZNep was a more potent inhibitor of human AdoHcy hydrolase, about 40-fold more potent, than DZNari (Table 1), and resulted in higher AdoHcy levels than observed for DZNari. While the incorporation of [ $^{35}\text{S}$ ]methionine into AdoHcy increased with time, the untreated cells displayed a slight decline in the overall amount of [ $^{35}\text{S}$ ]AdoHcy.

In contrast to the AdoHcy results, cells treated with either DZNari or DZNep showed no significant difference in the level of [ $^{35}\text{S}$ ]AdoMet over 3 h. However, about 10-fold

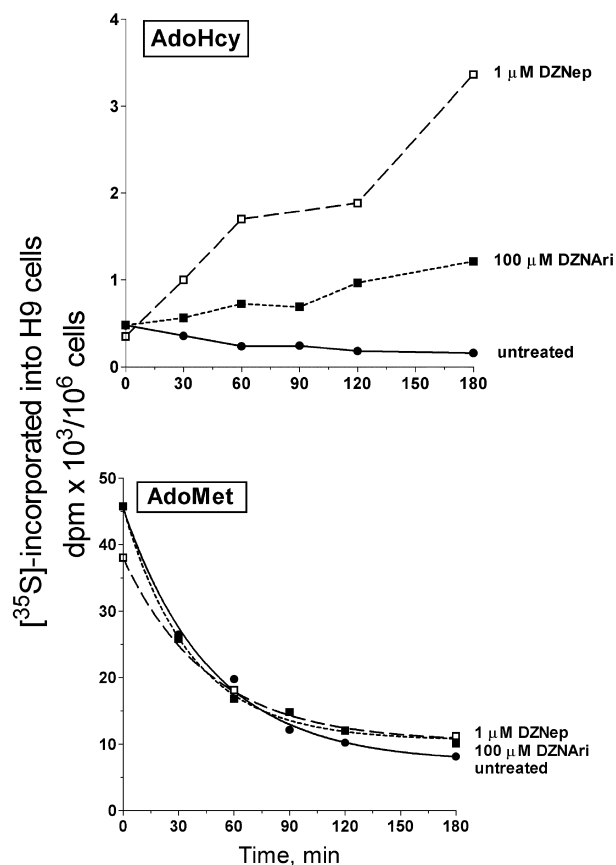


**Fig. 2.** AdoHcy (top), and AdoMet (bottom) levels in DZNari (100  $\mu\text{M}$ ) and DZNep (1  $\mu\text{M}$ ) treated H9 cells. Cells were prelabelled with [ $^{35}\text{S}$ ]methionine and then treated with drug; AdoMet and AdoHcy levels were determined as described in Materials and methods.

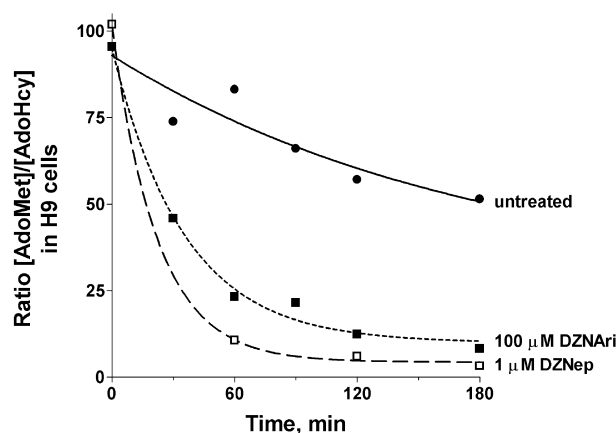


**Fig. 3.** Ratio of AdoMet/AdoHcy in H9 cells treated with DZNari (100  $\mu\text{M}$ ) or DZNep (1  $\mu\text{M}$ ).

more [ $^{35}\text{S}$ ]methionine was incorporated into AdoMet than AdoHcy (Fig. 2, bottom). This was not surprising as significant rises in the level of AdoHcy accompanied by minute changes in AdoMet have also been observed with other DZA analogs [3].

It is generally hypothesized that the extent of the inhibition of methylation reactions is inversely correlated with the AdoMet/AdoHcy ratio [1]. While it only required 1  $\mu\text{M}$  DZNep to produce a pronounced decrease in the AdoMet/AdoHcy ratio, a 100-fold higher concentration of DZNari (100  $\mu\text{M}$ ) was needed to achieve a similar decrease in this ratio (Fig. 3).

### Triphosphates of DZAri and DZNep

The cellular phosphorylation pathway for DZNep or DZAri to their respective nucleotides has not been elucidated, despite the report of the existence of the nucleotides of NepA, DZNep, and DZAri [10–12]. To further explore the mechanism by which these DZA analogs act as anti-HIV-1 agents, the possible formation of 3-deaza-nucleotides of DZNep and DZAri was examined in cells designed to be deficient in specific kinases. Both H9 and V79 (TK<sup>+</sup>) cells express the full complement of phosphorylating enzymes, while the AA-2 cells (AK<sup>-</sup>, dCK<sup>-</sup>) lack adenosine and deoxycytidine kinase [25] and V79 (TK<sup>-</sup>) cells lack thymidine kinase [26]. These kinases have been shown to be able to phosphorylate a variety of nucleosides. As shown in Table 2, the lack of adenosine and deoxycytidine kinase or thymidine kinase did not alter the amount of [ $^3\text{H}$ ]triphosphates of DZNep or DZAri formed. However, based on the

**Table 2.** Triphosphates of DZAri and DZNep in cells. Cells were incubated with [ $^3\text{H}$ ]DZAri or [ $^3\text{H}$ ]DZNep as described in Materials and methods for 18 h;  $n = 2$  for all cells except H9 cells, where  $n = 3$ . Values are given mean  $\pm$  SD in  $10^6$  pmol.

Cell type	[ $^3\text{H}$ ]DZAri-TP	[ $^3\text{H}$ ]DZNep-TP
H9	0.64 $\pm$ 0.07	0.25 $\pm$ 0.03
AA-2 (AK <sup>-</sup> , dCK <sup>-</sup> )	0.59 $\pm$ 0.09	0.28 $\pm$ 0.02
V79 (TK <sup>+</sup> )	3.4 $\pm$ 0.27	1.0 $\pm$ 0.05
V79 (TK <sup>-</sup> )	2.6 $\pm$ 0.10	1.4 $\pm$ 0.06

amount of 3-deaza-nucleotides formed (Table 2), the cells could be ranked for their efficiency in anabolically phosphorylating the 3-deaza-nucleosides: V79 (TK<sup>+</sup>)  $\approx$  V79 (TK<sup>-</sup>) > H9  $\approx$  AA-2. Although DZA has been shown to be phosphorylated by liver 5'-nucleotidase [14], no phosphorylated [<sup>3</sup>H]DZNep was detected when the DZNep was incubated with partially purified liver 5'-nucleotidase (data not shown). These results indicated that adenosine kinase, deoxycytidine kinase, and thymidine kinase were not important enzymes for the phosphorylation of DZNep or DZAri. To synthesize the nucleotides of DZNep or DZAri for direct testing on viral enzymes, the enzyme(s) responsible for phosphorylating these analogs need to be elucidated since no chemical synthesis is available.

### Anti-HIV-1 activity of the DZA analogs

The anti-HIV-1 effects of the DZA analogs and NepA were compared by their inhibition of HIV-1 p24 antigen production in PBMCs infected with HIV-1 strains A012 and A018 [37,38], both of which were obtained from AZT-naive individuals (Table 1). For the purpose of comparison, the reported IC<sub>50</sub> values for AZT were 0.02 and 0.03  $\mu$ M for the A012 and A018 strains, respectively [10]. With respect to the A018 strain, DZNep and NepA were the most potent inhibitors of HIV-1 p24 antigen production, yielding IC<sub>50</sub> values of 0.016 and 0.018  $\mu$ M, respectively. DZAri and DZA showed similar IC<sub>50</sub> values of 0.22 and 0.20  $\mu$ M, respectively. DZNari, modified from DZAri and theoretically not able to be phosphorylated because of the missing 5'-hydroxyl group, was 25- and 13-fold less potent than the parent compound DZAri for the two strains. The dideoxy analogs, ddDZA and ddDZAri, were almost equal in their activity, but were about 10-fold less potent than their respective parent dioxy-compounds (Table 1). ddAdo was twofold less potent than the two other dideoxy 3-deaza analogs (IC<sub>50</sub> = 4.8  $\mu$ M), and similar IC<sub>50</sub> values were observed for the A012 strain.

### Correlation of anti-HIV-1 activity and inhibition of AdoHcy hydrolase

Figure 4 shows the correlation of the log of the IC<sub>50</sub> values for the inhibition of p24 antigen in PBMC (*y*-axis) infected with HIV-1 strains A012 and A018 and the log of the K<sub>i</sub> values for the inhibition of the placental AdoHcy hydrolase (*x*-axis). Linear regression analysis yielded an *r*<sup>2</sup> value of 0.8 for both strains of HIV-1. In comparison, when DZNari was omitted from the analysis, the *r*<sup>2</sup> value became 0.9 for both strains. The 95% confidence limits for all the DZA analogs are shown by the dotted lines. Only DZNari was outside of the 95% confidence limits of the regression line. Therefore, the deletion of the methylene group from DZAri to yield DZNari, now containing a secondary hydroxyl group, led to a threefold reduction in the K<sub>i</sub> for the inhibition of AdoHcy hydrolase and a corresponding 25- and 13-fold decrease in the inhibition of HIV-1 A012 and A018 p24 antigen in PBMC, respectively. These results indicated that the inhibition of AdoHcy hydrolase alone was not enough to fully account for the anti-HIV activity of the DZA analogs.

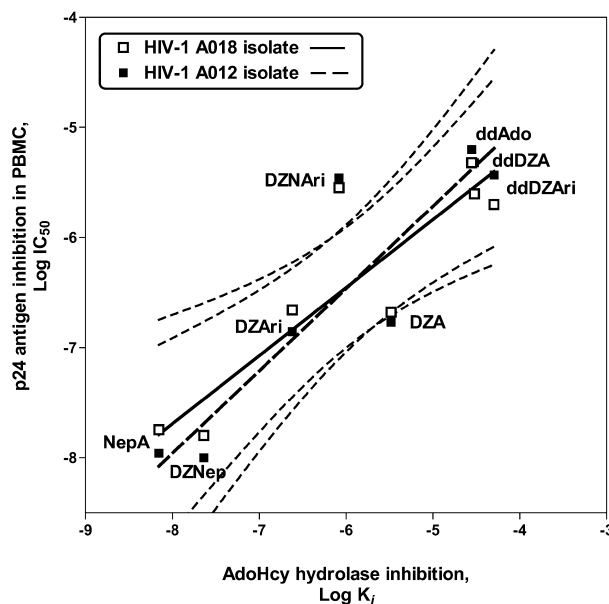


Fig. 4. Correlation between the K<sub>i</sub> values for the inhibition of human placental AdoHcy hydrolase and the log of the IC<sub>50</sub> values (Table 1) for the inhibition of p24 antigen by HIV-1 isolates A012 and A018 in PHA-stimulated PBMC. Dashed lines denote the 95% confidence limit.

### MM-based models for AdoHcy hydrolase inhibition: correlation of theoretical binding energies and experimental K<sub>i</sub> values

To generate a QSAR-like model for the potency of inhibition of human AdoHcy hydrolase by the DZA analogs, the energy of binding between the analogs and the enzyme were calculated using the MM-based approach [35]. Each analog was docked in the AdoHcy hydrolase active-site; the initial 3D models were based on the available crystallographic structures [28,29]. Figure 5 illustrates the 3D model for the complex of NepA bound to the active site of AdoHcy. The side-chains of AdoHcy participating in hydrogen bonding (violet dashed lines) with NepA are represented as sticks. With the exception of the dideoxy deaza analogs, this hydrogen bond pattern is common for all of the potent DZA analogs. The extensive hydrogen bonding with the 2'-OH and 3'-OH of the ribose moiety can explain the loss of activity of the dideoxy DZA analogs as observed in Fig. 4. Thus, the difference in the potency of the DZA analogs probably involves other factors including hydrophobic contacts and extent of the contact surface area. More sophisticated techniques will have to be applied to determine their individual contribution to the strength of binding. In addition, some analogs differ in their sugar conformation in comparison to adenosine (Fig. 1).

Two simple models, a basic and extended, were developed for calculating the energy of binding for the DZA analogs.

**Basic model.** For the basic model, which lacks the solvent effects, a good linear correlation was found between the calculated binding energies (kcal·mol<sup>-1</sup>) and the log of the K<sub>i</sub> values for hydrolase inhibition (Fig. 6, bottom). A regression coefficient of *r*<sup>2</sup> = 0.93 was obtained for AdoHcy hydrolase inhibition. When the protein energy

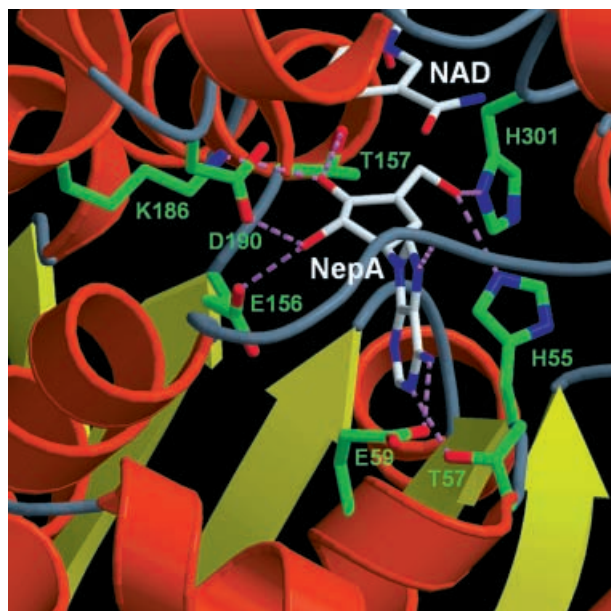


Fig. 5. 3D model for NepA–NAD–AdoHcy hydrolase complex. The side-chains of AdoHcy participating in hydrogen bonding (violet dashed lines) with NepA are represented as sticks.

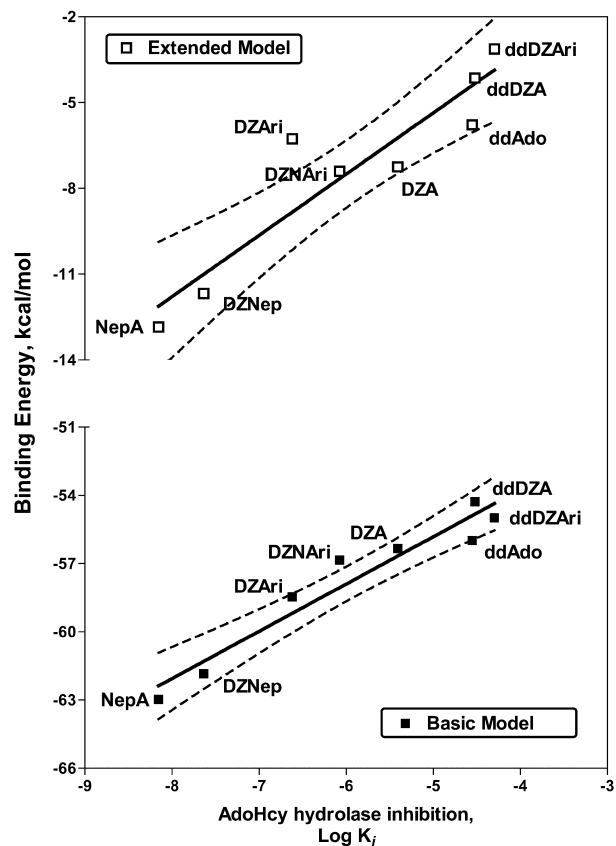


Fig. 6. Linear correlation between the theoretical binding energy and the  $\log K_i$  for basic model with averaged protein energy (bottom), and extended model with single molecule protein energy (top). Dashed lines denote the 95% confidence limit.

was averaged for all the compounds, an  $r^2 = 0.93$  was obtained. In comparison, an  $r^2 = 0.89$  was found for a single molecule protein energy. In the latter case, DZA was a clear outlier (not shown). However, it should be noted that the AdoHcy hydrolase–DZA cocystal structure was used as a template to build the 3D models of complexes with the remaining DZA analogs. Therefore, it was likely that the interactions with DZA were particularly favorable, biasing results in a direction of improved DZA binding. This effect could be partially offset by averaging the protein energy, which might account for the slightly better results of the averaged model. When the correlation analysis excluded DZA, the correlation coefficient for the averaged model remained unchanged ( $r^2 = 0.93$ ), whereas the correlation for the single molecule protein energy model was surprisingly high ( $r^2 = 0.99$ , data not shown).

**Extended model.** In the extended model, the surface energy term containing the proportionality coefficient  $k_s = -0.09 \text{ kcal}\cdot\text{mol}^{-1}\cdot\text{Å}^{-2}$  was used to account for the averaged interactions with solvent. By this approach, the correlation between the  $\log K_i$  values of the DZA inhibitors and the predicted binding energy decreased. When the protein energy was averaged over all the compounds, an  $r^2 = 0.51$  was obtained (not shown), while an  $r^2 = 0.86$  was obtained for a single molecule protein energy. However, the predicted binding energies decreased dramatically from in the range  $-64$  to  $-52 \text{ kcal}\cdot\text{mol}^{-1}$  for the basic model (Fig. 6, bottom) to a more reasonable range of  $-14$  to  $-2 \text{ kcal}\cdot\text{mol}^{-1}$  for the extended model (Fig. 6, top), which incorporates the surface term.

Computation of the energy of binding in the basic model takes about 15 min for each compound on the SGI O2 workstation; an additional 2 min are required for computing the surface. Calculation of the free energy of binding, with the free energy perturbation or thermodynamical integration methods, would require long molecular dynamics simulations, that would take at least two orders of magnitude longer.

## Discussion

The present investigations elaborate on the mechanism of action of the DZA analogs as anti-HIV-1 agents. First, eight adenosine analogs (Fig. 1) were examined for their inhibitory effect on human placental AdoHcy hydrolase. The ability of this and similar compounds to block both RNA and DNA viruses has been attributed to the inhibition of cellular *S*-adenosylhomocysteine hydrolase because the enzyme is not expressed by the virus [1,9,10,18]. The order of potency was  $\text{NepA} \approx \text{DZNep} \gg \text{DZAri} \approx \text{DZNAri} > \text{DZA} \gg \text{ddAdo} \approx \text{ddDZA} \approx \text{ddDZari}$  (Table 1). The ddDZA and ddDZari analogs were among the least potent human hydrolase inhibitors. A similar rank order of potency for NepA, DZNep, DZAri and DZA as observed here was also found for the inhibition of AdoHcy hydrolase from liver [27].

The same DZA analogs were then tested for their anti-HIV-1 activities. With the exception of DZNAri, the only compound with a secondary hydroxyl group that precludes phosphorylation [17], NepA, DZNep, DZAri, and DZA were all potent inhibitors of p24 antigen production by the

AZT-sensitive HIV-1 strains, A012 and A018 (Table 1). The poor efficacy of DZNAri was in agreement with a report that it was ineffective in inhibiting HIV-1 strain III<sub>B</sub> in CEM cell cultures [18]. The three dideoxy compounds also displayed poor anti-HIV-1 potency. In contrast to the potent anti-HIV-1 activity of other types of dideoxy nucleosides, the conversion of the DZA analogs to their dideoxy derivatives, ddDZA and ddDZAr, did not improve upon the anti-HIV activity of DZA or DZAr. Indeed, ddDZA and ddDZAr were markedly less potent than their parent compounds. The order of potency for the inhibition of p24 antigen for either of the A012 or A018 isolates was: DZNep  $\approx$  NepA  $\gg$  DZAr  $\approx$  DZA  $\gg$  ddDZAr  $\approx$  ddDZA  $\approx$  DZNAri  $\approx$  ddAdo.

A linear correlation was established between the log IC<sub>50</sub> values for inhibition of p24 antigen production by both HIV-1 A012 and A018 isolates in PBMC and the log K<sub>i</sub> values for inhibition of human placental AdoHcy hydrolase (Fig. 4). The coefficient of correlation ( $r^2$ ) was 0.9 for both A012 and A018 strains when DZNAri was excluded from the analysis. In comparison, the  $r^2$  value was reduced to 0.8 when DZNAri was included in the linear regression analysis. DZNAri was the only compound to fall outside the 95% confidence limit for each HIV-1 strain, and the only compound unlikely to be phosphorylated *in vitro*. Thus, this result suggests an additional requirement of the DZA analogs to exhibit potent antiviral activity against HIV-1: there must be a cellular processing of the DZA nucleoside analog to form the phosphorylated analog.

AdoHcy is the most important regulator of methylation-dependent events [1,4,39]. As the AdoMet/AdoHcy ratio decreases (Figs 2 and 3), the inhibition of methylation processes presumably increases. In H9 cells treated with DZNep and DZNAri, the AdoMet/AdoHcy ratio markedly decreased compared to untreated cells (Figs 2 and 3), indicating a possible inhibition of cellular methylation(s). Also, DZNep was more potent than DZNAri both in inhibiting AdoHcy hydrolase (Table 1) and in decreasing the AdoMet/AdoHcy ratio. In another cell system, the AdoMet/AdoHcy ratio for DZAr has been reported to fall between DZNep and DZNAri [3], and DZAr is intermediate in potency in the hydrolase inhibition assay (Table 1).

Most likely, several mechanisms contribute to the unique antiviral activity of the DZA analogs. As AdoHcy hydrolase inhibitors, DZA and DZAr have been shown to decrease the AdoMet/AdoHcy ratio and inhibit methylation of DNA, RNA, protein, lipid, and small molecules, and affect cell gene activation [40–44]. The replication of influenza virus was affected differentially by NepA and DZA; NepA apparently perturbed viral transcription by a mechanism not involving an accumulation of AdoHcy [45].

The difference in the anti-HIV-1 efficacy of DZAr and DZNAri can be explained, at least partly, by a difference in their metabolism. DZNAri should be resistant to adenosine deaminase because it also contains the 3-deaza-adenine moiety [1]. Unlike DZAr or DZNep, which undergoes phosphorylation at the 5' position [10], DZNAri contains a secondary hydroxyl group and is not a substrate for cellular kinases [17]. It has been shown that several DZA analogs could be converted to their nucleotide derivatives

[5,10,12,14], although the cellular kinases involved have not been completely elucidated. It has been reported that DZA is capable of being phosphorylated by rat liver 5'-nucleotidase [14]. Although nucleotides of [<sup>3</sup>H]DZNep incubated similarly with this partially purified enzyme were not detected in our studies, H9 cell supernatants yielded the DZNep nucleotides (not shown). Also, it was reported that the RB<sup>R</sup>-1 CHO cell line, deficient only in adenosine kinase, failed to phosphorylate NepA [11]. Our results (Table 2) demonstrated that AA-2 cells, verified to be deficient in adenosine kinase, exhibited no decrease in the phosphorylation of either [<sup>3</sup>H]DZNep or [<sup>3</sup>H]DZAr. Therefore, part of the mode of action of these analogs might be similar to that of AZT, which is converted by cellular kinases to AZT triphosphate, and then suppresses HIV-1 replication by inhibiting viral reverse transcriptase, inducing chain termination, and perhaps by interacting with other viral enzymes such as integrase or perturbing host metabolism. The cytotoxic effects of these nucleosides have been suggested to be a result of nucleotides formed by cellular kinase(s) [15], and also functional AdoHcy hydrolase is necessary for survival, as demonstrated by mouse embryo death after deletion of the AdoHcy hydrolase gene [46]. We have shown that DZAr and DZNep could undergo anabolic phosphorylation in cells that are TK, or AK and dCK deficient (Table 2). As the kinases that phosphorylate the deaza- compounds (i.e. the sequence of mono-, di-, and finally tri-phosphate) remain to be elucidated, it is also not known whether the different rates of anabolic phosphorylation of each deaza-analog contribute to their anti-HIV activity. Indeed, the ratio of DZAr nucleotides (mono/di/tri) were not equimolar to those observed for DZNep (not shown).

Our results presented here implicate a dual mechanism by which the deaza-analogs, with the exception of DZNAri, inhibit p24 antigen production. For instance, both DZA and DZAr exhibit similar anti-HIV potency (Table 1), but DZAr is a more potent hydrolase inhibitor. These results may reflect the efficiency of the phosphorylation process in different cells, the potency of the respective phosphorylated analogs, the direct inhibition of AdoHcy hydrolase by DZAr or DZA, and the inhibition of AdoMet-dependent methyltransferases by DZAHcy formed by conjugation with cellular homocysteine, which may not occur to the same extent with DZAr. While some of the DZA compounds are potent AdoHcy hydrolase inhibitors (Table 1), they are also phosphorylated to nucleotides in cells (with the significant exception of DZNAri). However, there has been no evaluation of the effect of the phosphate analogs of DZA-nucleotides as substrate or inhibitors of ATP:L-methionine-S-adenosyltransferase (AdoMet synthetase). It can not be predicted whether deaza-nucleotides would alter AdoMet synthetase activity based on the potency of ATP and ADP derivatives to act as substrates or inhibitors of AdoMet synthetase [47], and that adenine and ribose moieties have minor contacts compared to the phosphate groups with the enzyme active site [48,49]. As DZAr has been shown to inhibit AdoMet decarboxylase in HeLa cell extracts [50], it is likely that other DZA analogs also affect the AdoMet decarboxylase. This enzyme provides decarboxylated AdoMet, an essential precursor to all polyamine biosynthesis. Finally, monophosphates have

been reported to bind to and inactivate *S*-adenosylhomocysteine hydrolase, although the potency was significantly decreased over that of the parent nucleoside [51]. Thus, there could be a more complex synergistic interaction (than proposed here) between a DZA analog, its nucleotide(s), methionine-*S*-adenosyltransferase, AdoHcy hydrolase, and other AdoMet related cycles such as polyamine biosynthesis. It is possible that all these interactions contribute to the antiviral potency of the deaza-analogs.

During the past 6 years, several structures of human and rat AdoHcy hydrolase have been solved and a detailed catalytic mechanism proposed [28,29,52–54]. Comparison of AdoHcy hydrolase complexes with adenosine [29], 3'-oxo-adenosine [54], 2'-hydroxy,3'-ketocyclopent-4'-enyladenine [28], and D-eritadenine [53] revealed the common, single binding mode and showed that the active site is relatively rigid in nature. Taking into account these observations, the currently available AdoHcy hydrolase structures provide a very good basis for modeling other adenosine analog complexes.

To provide a tool for the fast and effective screening of new adenosine derivatives for AdoHcy hydrolase inhibition, two theoretical, QSAR-like, models for predicting binding energies were developed here, based on the linear interaction energy approach. Both models allowed for reasonably accurate estimations of potency of inhibition for experimentally tested adenosine analogs, notwithstanding the small differences between the ligands. In comparison to the more sophisticated and accurate free energy methods that are computationally very intensive, our approach is very fast, and practical applications are not limited by computational costs. To even further simplify this methodology and reducing the most computationally demanding step of this procedure, a charge equilibration estimation was used instead of computing electrostatic potential charges with quantum-mechanical methods. The excellent correlation of the calculated binding energies with the experimental data suggests that these models can be used for effective screening of new adenosine analogs with similar binding modes. Thus, more potent AdoHcy hydrolase inhibitors could be predicted. In the basic model, all solvent effects were neglected; nevertheless, this approach gave excellent correlations with experimental AdoHcy hydrolase inhibition. However, the estimated binding energies are nonphysically large when comparing to realistic free energy values. There are two major sources for this discrepancy. One can be related to the neglected interactions of the molecular system with the solvent, another to lack of the scaling applied in the linear interaction energy model, where the resulting energies are scaled between 0.144 and 0.5, depending on the model variant and type of interactions. The extended model was introduced to find out if addition of the term, proportional to the surface, that mimics interactions with the solvent, could improve the results. In this model predicted binding energies improved significantly, but the correlation between the  $K_i$  for AdoHcy hydrolase inhibition and the binding energy was reduced in the averaged model. Therefore, it can be concluded that discrepancies between a realistic energy scale and results obtained with the basic model are due to the lack of the scaling and interactions with the solvent. Nevertheless, the basic model, which

does not contain any adjustable parameters, can be used for predicting relative binding affinities for a series of compounds.

Recently, the crystal structure of AdoHcy hydrolase complexed with NepA and NAD molecules was solved [19], enabling a rigorous verification of our modeling approach. As assumed in our study that analyzed adenosine analogs bind in a single, well defined conformation, the binding of NepA [19] and 2'-hydroxy,3'-ketocyclopent-4'-enyladenine [28] in a tight binding pocket of AdoHcy hydrolase are virtually identical. The superposition of all C $\alpha$  atoms of the modeled and the experimental structure of NepA–AdoHcy hydrolase complexes results in rms deviation of 0.37 Å and in NepA molecules fitting almost perfectly (Fig. 7). The active site side-chain rotamers are predicted correctly to allow reproducing all the protein–ligand interactions. The main difference comes from the position of O5' of NepA that in the modeled structure makes a relatively weaker hydrogen bond with the Asp131 side chain than in the crystal structure. Confirmation of the correctness of our molecular mechanics based model for the enzyme–NepA complex by the crystallographic studies makes it reasonable to expect that the remaining AdoHcy hydrolase–adenosine analog complexes were also modeled correctly.

In conclusion, the DZA analogs could exert their anti-HIV-1 effect via a combination, at the very least, of 3-deaza-nucleotides, that might inhibit reverse transcriptase or integrase, and the inhibition of viral or cellular methylation reactions. Elucidation of the cellular phosphorylation pathway could result in the enzymatic synthesis of the nucleotides, allowing direct testing of the 3-deaza-nucleotides on viral and cellular enzymes. Taking into account the importance of AdoHcy hydrolase inhibition for viral therapy, application of our theoretical approach for the fast and effective screening of new adenosine analogs that

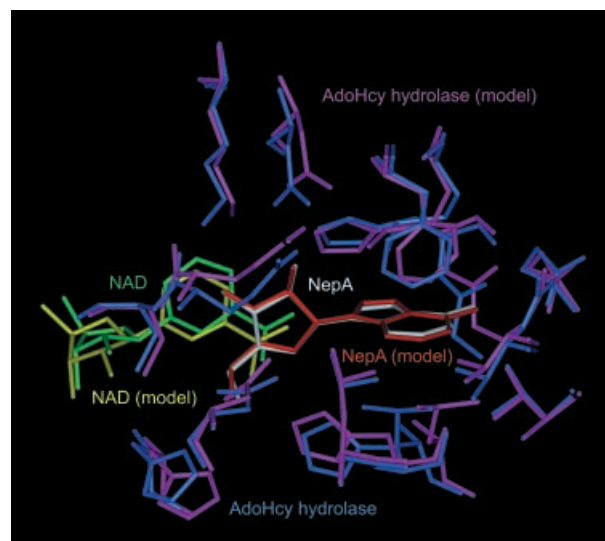


**Fig. 7. Comparison of 3D model and recently solved crystal structure of NepA–NAD–AdoHcy hydrolase complex (1LJ4).** Active site residues within 4 Å from NepA as well as part of NAD molecule are shown only. AdoHcy hydrolase is colored in violet and blue, NAD in yellow and green, NepA in red and white for the 3D model and experimental structure, respectively.

can be metabolically converted to their respective nucleotides could result in predicting more potent antiviral agents.

## Acknowledgements

J. M. B. is an EMBO Young Investigator and an EMBO and HHMI Scientist.

## References

- Chiang, P.K. (1998) Biological effects of inhibitors of *S*-adenosylhomocysteine hydrolase. *Pharmacol. Ther.* **77**, 115–134.
- Glazer, R.I., Hartman, K.D., Knode, M.C., Richard, M.M., Chiang, P.K., Tseng, C.K. & Marquez, V.E. (1986) 3-Deazaneplanocin: a new and potent inhibitor of *S*-adenosylhomocysteine hydrolase and its effects on human promyelocytic leukemia cell line HL-60. *Biochem. Biophys. Res. Commun.* **135**, 688–694.
- Aarbakke, J., Miura, G.A., Prytz, P.S., Bessesen, A., Slordal, L., Gordon, R.K. & Chiang, P.K. (1986) Induction of HL-60 cell differentiation by 3-deaza-(±)-aristeromycin, an inhibitor of *S*-adenosylhomocysteine hydrolase. *Cancer Res.* **46**, 5469–5472.
- Chiang, P.K., Gordon, R.K., Tal, J., Zeng, G.C., Doctor, B.P., Pardhasaradhi, K. & McCann, P.P. (1996) *S*-adenosylmethionine and methylation. *FASEB J.* **10**, 471–480.
- Liu, S., Wolfe, M.S. & Borchardt, R.T. (1992) Rational approaches to the design of antiviral agents based on *S*-adenosyl-L-homocysteine hydrolase as a molecular target. *Antiviral Res.* **19**, 247–265.
- Snoeck, R., Andrei, G., Neyts, J., Schols, D., Cools, M., Balzarini, J. & De Clercq, E. (1993) Inhibitory activity of *S*-adenosylhomocysteine hydrolase inhibitors against human cytomegalovirus replication. *Antiviral Res.* **21**, 197–216.
- Prigge, S.T. & Chiang, P.K. (2001) *Homocysteine in Health and Disease*. Cambridge University Press, Cambridge, UK.
- Bourdais, J., Biondi, R., Sarfati, S., Guerreiro, C., Lascu, I., Janin, J. & Veron, M. (1996) Cellular phosphorylation of anti-HIV nucleosides. Role of nucleoside diphosphate kinase. *J. Biol. Chem.* **271**, 7887–7890.
- Placidi, L., Cretton-Scott, E., Gosselin, G., Pierra, C., Schinazi, R.F., Imbach, J.L., el Kouni, M.H. & Sommadossi, J.P. (2000) Intracellular metabolism of beta-L-2',3'-dideoxyadenosine: relevance to its limited antiviral activity. *Antimicrob. Agents Chemother.* **44**, 853–858.
- Mayers, D.L., Mikovits, J.A., Joshi, B., Hewlett, I.K., Estrada, J.S., Wolfe, A.D., Garcia, G.E., Doctor, B.P., Burke, D.S., Gordon, R.K., Lane, J.R. & Chiang, P.K. (1995) Anti-human immunodeficiency virus 1 (HIV-1) activities of 3-deazaadenosine analogs: increased potency against 3'-azido-3'-deoxythymidine-resistant HIV-1 strains. *Proc. Natl Acad. Sci. USA* **92**, 215–219.
- Saunders, P.P., Tan, M.T. & Robins, R.K. (1985) Metabolism and action of neplanocin A in Chinese hamster ovary cells. *Biochem. Pharmacol.* **34**, 2749–2754.
- Whaun, J.M., Miura, G.A., Brown, N.D., Gordon, R.K. & Chiang, P.K. (1986) Antimalarial activity of neplanocin A with perturbations in the metabolism of purines, polyamines and *S*-adenosylmethionine. *J. Pharmacol. Exp. Ther.* **236**, 277–283.
- Bennett, L.L. Jr, Bowdon, B.J., Allan, P.W. & Rose, L.M. (1986) Evidence that the carbocyclic analog of adenosine has different mechanisms of cytotoxicity to cells with adenosine kinase activity and to cells lacking this enzyme. *Biochem. Pharmacol.* **35**, 4106–4109.
- Prus, K.L., Wolberg, G., Keller, P.M., Fyfe, J.A., Stopford, C.R. & Zimmerman, T.P. (1989) 3-Deazaadenosine 5'-triphosphate: a novel metabolite of 3-deazaadenosine in mouse leukocytes. *Biochem. Pharmacol.* **38**, 509–517.
- Glazer, R.I. & Knode, M.C. (1984) Neplanocin A. A cyclopentenyl analog of adenosine with specificity for inhibiting RNA methylation. *J. Biol. Chem.* **259**, 12964–12969.
- Montgomery, J.A., Clayton, S.J., Thomas, H.J., Shannon, W.M., Arnett, G., Bodner, A.J., Kion, I.K., Cantoni, G.L. & Chiang, P.K. (1982) Carbocyclic analogue of 3-deazaadenosine: a novel antiviral agent using *S*-adenosylhomocysteine hydrolase as a pharmacological target. *J. Med. Chem.* **25**, 626–629.
- Iltzsch, M.H., Uber, S.S., Tankersley, K.O. & el Kouni, M.H. (1995) Structure–activity relationship for the binding of nucleoside ligands to adenosine kinase from *Toxoplasma gondii*. *Biochem. Pharmacol.* **49**, 1501–1512.
- Siddiqi, S.M., Chen, X., Rao, J., Schneller, S.W., Ikeda, S., Snoeck, R., Andrei, G., Balzarini, J. & De Clercq, E. (1995) 3-deaza- and 7-deaza-5'-noraristeromycin and their antiviral properties. *J. Med. Chem.* **38**, 1035–1038.
- Yang, X., Hu, Y., Yin, D.H., Turner, M.A., Wang, M., Borchardt, R.T., Howell, P.L., Kuczera, K. & Schowen, R.L. (2003) Catalytic strategy of *S*-adenosyl-L-homocysteine hydrolase: transition-state stabilization and the avoidance of abortive reactions. *Biochemistry* **42**, 1900–1909.
- Franchetti, P., Cappellacci, L., Cristalli, G., Grifantini, M., Pani, A., La Colle, P. & Nocentini, G. (1991) Synthesis and evaluation of anti-HIV and antitumor activity of 2',3'-dideoxy-2',3'-dideoxy-3-deaza-adenosine, 2',3'-dideoxy-3-deaza-adenosine, and some 2',3'-dideoxy-3-deaza-adenosine 5'-dialkyl phosphates. *Nucleosides Nucleotides* **10**, 1551–1562.
- Robins, M.J., Madej, D., Low, N.H., Hansske, F. & Zou, R. (1991) 2',3'-Dideoxyadenosine and 2,6-diamino-9-(2,3-dideoxy-β-D-glycero-pentofuranosyl) purine: Efficient conversion of ribonucleosides into their 2',3'-dideoxy derivatives via their 2',3'-unsaturated counterparts. In *Nucleic Acid Chemistry: Improved and New Synthetic Procedures, Methods, and Techniques* (Townsend, L.B. & Tipson, R.S., eds), pp. 211–219. Wiley Interscience, New York.
- Hershfield, M.S., Aiyar, V.N., Premakumar, R. & Small, W.C. (1985) *S*-Adenosylhomocysteine hydrolase from human placenta. Affinity purification and characterization. *Biochem. J.* **230**, 43–52.
- Guranowski, A., Montgomery, J.A., Cantoni, G.L. & Chiang, P.K. (1981) Adenosine analogues as substrates and inhibitors of *S*-adenosylhomocysteine hydrolase. *Biochemistry* **20**, 110–115.
- Japour, A.J., Mayers, D.L., Johnson, V.A., Kuritzkes, D.R., Beckett, L.A., Arduino, J.M., Lane, J., Black, R.J., Reichelderfer, P.S. & D'Aquila, R.T. (1993) Standardized peripheral blood mononuclear cell culture assay for determination of drug susceptibilities of clinical human immunodeficiency virus type 1 isolates. The RV-43 Study Group, the AIDS Clinical Trials Group Virology Committee Resistance Working Group. *Antimicrob. Agents Chemother.* **37**, 1095–1101.
- Chaffee, S., Leeds, J.M., Matthews, T.J., Weinhold, K.J., Skinner, M., Bolognesi, D.P. & Hershfield, M.S. (1988) Phenotypic variation in the response to the human immunodeficiency virus among derivatives of the CEM T and WIL-2 B cell lines. *J. Exp. Med.* **168**, 605–621.
- Nyce, J., Leonard, S., Canupp, D., Schulz, S. & Wong, S. (1993) Epigenetic mechanisms of drug resistance: drug-induced DNA hypermethylation and drug resistance. *Proc. Natl Acad. Sci. USA* **90**, 2960–2964.
- Chiang, P.K. & Miura, G.A. (1986) *S*-Adenosylhomocysteine hydrolase. In *Biological Methylation and Drug Design* (Borchardt, R.T., Creveling, C.R. & Ueland, P.M., eds), pp. 239–251. Humana Press, New Jersey.
- Turner, M.A., Yuan, C.S., Borchardt, R.T., Hershfield, M.S., Smith, G.D. & Howell, P.L. (1998) Structure determination of selenomethionyl *S*-adenosylhomocysteine hydrolase using data at a single wavelength. *Nat. Struct. Biol.* **5**, 369–376.

29. Komoto, J., Huang, Y., Gomi, T., Ogawa, H., Takata, Y., Fujioka, M. & Takusagawa, F. (2000) Effects of site-directed mutagenesis on structure and function of recombinant rat liver *S*-adenosylhomocysteine hydrolase. Crystal structure of D244E mutant enzyme. *J. Biol. Chem.* **275**, 32147–32156.
30. Hwang, M.-J., Stockfisch, T.P. & Hagler, A.T. (1994) Derivation of class II force fields. II. Derivation and characterization of a class II force field, CFF93, for the alkyl functional group and alkane molecules. *J. Am. Chem. Soc.* **116**, 2515–2525.
31. Maple, J.R., Hwang, M.-J., Stockfisch, T.P., Dinur, U., Waldman, M., Ewig, C.S. & Hagler, A.T. (1994) Derivation of class II force fields. I. Methodology and quantum force field for the alkyl functional group and alkane molecules. *J. Comput. Chem.* **15**, 162–182.
32. Rappe, A.K. & Goddard, W.A.I. (1991) Charge equilibration for molecular dynamics simulations. *J. Phys. Chem.* **95**, 3358–3363.
33. Aqvist, J., Medina, C. & Samuelsson, J.E. (1994) A new method for predicting binding affinity in computer-aided drug design. *Protein Eng.* **7**, 385–391.
34. Hansson, T., Marelus, J. & Aqvist, J. (1998) Ligand binding affinity prediction by linear interaction energy methods. *J. Comput. Aided Mol. Des.* **12**, 27–35.
35. Rudnicki, W.R., Kurzepa, M., Szczepanik, T., Priebe, W. & Lesyng, B. (2000) A simple model for predicting the free energy of binding between anthracycline antibiotics and DNA. *Acta Biochim. Pol.* **47**, 1–9.
36. Hubbard, S.J. & Thornton, J.M. (1993) *NACCESS, Computer Program*. Department of Biochemistry and Molecular Biology, University College London, <http://wolf.bms.umist.ac.uk/naccess/>.
37. Johnson, V.A., Merrill, D.P., Chou, T.C. & Hirsch, M.S. (1992) Human immunodeficiency virus type 1 (HIV-1) inhibitory interactions between protease inhibitor Ro 31-8959 and zidovudine, 2',3'-dideoxycytidine, or recombinant interferon-alpha A against zidovudine-sensitive or -resistant HIV-1 *in vitro*. *J. Infect. Dis.* **166**, 1143–1146.
38. Larder, B.A., Darby, G. & Richman, D.D. (1989) HIV with reduced sensitivity to zidovudine (AZT) isolated during prolonged therapy. *Science* **243**, 1731–1734.
39. Greenberg, M.L., Chaffee, S. & Hershfield, M.S. (1989) Basis for resistance to 3-deazaaristeromycin, an inhibitor of *S*-adenosylhomocysteine hydrolase, in human B-lymphoblasts. *J. Biol. Chem.* **264**, 795–803.
40. Backlund, P.S. Jr, Carotti, D. & Cantoni, G.L. (1986) Effects of the *S*-adenosylhomocysteine hydrolase inhibitors 3-deazaadenosine and 3-deazaaristeromycin on RNA methylation and synthesis. *Eur. J. Biochem.* **160**, 245–251.
41. Chiang, P.K., Burbelo, P.D., Brugh, S.A., Gordon, R.K., Fukuda, K. & Yamada, Y. (1992) Activation of collagen IV gene expression in F9 teratocarcinoma cells by 3-deazaadenosine analogs. Indirect inhibitors of methylation. *J. Biol. Chem.* **267**, 4988–4991.
42. Liotta, L.A., Mandler, R., Murano, G., Katz, D.A., Gordon, R.K., Chiang, P.K. & Schiffmann, E. (1986) Tumor cell autocrine motility factor. *Proc. Natl Acad. Sci. USA* **83**, 3302–3306.
43. Smith, J.D. & Ledoux, D.N. (1990) Effect of the methylation inhibitors 3-deazaadenosine and 3-deazaaristeromycin on phosphatidylcholine formation in *Tetrahymena*. *Biochim. Biophys. Acta* **1047**, 290–293.
44. Wu, S., Liu, X., Solorzano, M.M., Kwock, R. & Avramis, V.I. (1995) Development of zidovudine (AZT) resistance in Jurkat T cells is associated with decreased expression of the thymidine kinase (TK) gene and hypermethylation of the 5' end of human TK gene. *J. Acquir. Immune. Defic. Syndr. Hum. Retrovirol.* **8**, 1–9.
45. Woyciniuk, P., Linder, M. & Scholtissek, C. (1995) The methyltransferase inhibitor Neplanocin A interferes with influenza virus replication by a mechanism different from that of 3-deazaadenosine. *Virus Res.* **35**, 91–99.
46. Miller, M.W., Duhl, D.M., Winkes, B.M., Arredondo-Vega, F., Saxon, P.J., Wolff, G.L., Epstein, C.J., Hershfield, M.S. & Barsh, G.S. (1994) The mouse lethal nonagouti a(x) mutation deletes the *S*-adenosylhomocysteine hydrolase (*Ahcy*) gene. *EMBO J.* **13**, 1806–1816.
47. Kappler, F., Hai, T.T. & Hampton, A. (1986) Isozyme-specific enzyme inhibitors. 10. Adenosine 5'-triphosphate derivatives as substrates or inhibitors of methionine adenosyltransferases of rat normal and hepatoma tissues. *J. Med. Chem.* **29**, 318–322.
48. Ma, Q.F., Kenyon, G.L. & Markham, G.D. (1990) Specificity of *S*-adenosylmethionine synthetase for ATP analogues mono- and disubstituted in bridging positions of the polyphosphate chain. *Biochemistry* **29**, 1412–1416.
49. Takusagawa, F., Kamitori, S. & Markham, G.D. (1996) Structure and function of *S*-adenosylmethionine synthetase: crystal structures of *S*-adenosylmethionine synthetase with ADP, BrADP, and PPI at 28 angstroms resolution. *Biochemistry* **35**, 2586–2596.
50. Gordon, R.K., Brown, N.D. & Chiang, P.K. (1983) Inhibition of adenosylmethionine decarboxylase and perturbation of polyamine metabolism by 3-deaza-(±) aristeromycin. *Biochem. Biophys. Res. Commun.* **114**, 505–510.
51. Helland, S. & Ueland, P.M. (1981) Interaction of 9-β-D-arabinofuranosyladenine, 9-β-D-arabinofuranosyladenine 5'-monophosphate, and 9-β-D-arabinofuranosyladenine 5'-triphosphate with *S*-adenosylhomocysteinase. *Cancer Res.* **41**, 673–678.
52. Hu, Y., Komoto, J., Huang, Y., Gomi, T., Ogawa, H., Takata, Y., Fujioka, M. & Takusagawa, F. (1999) Crystal structure of *S*-adenosylhomocysteine hydrolase from rat liver. *Biochemistry* **38**, 8323–8333.
53. Huang, Y., Komoto, J., Takata, Y., Powell, D.R., Gomi, T., Ogawa, H., Fujioka, M. & Takusagawa, F. (2002) Inhibition of *S*-adenosylhomocysteine hydrolase by acyclic sugar adenosine analogue D-eritadenine. Crystal structure of *S*-adenosylhomocysteine hydrolase complexed with D-eritadenine. *J. Biol. Chem.* **277**, 7477–7482.
54. Takata, Y., Yamada, T., Huang, Y., Komoto, J., Gomi, T., Ogawa, H., Fujioka, M. & Takusagawa, F. (2002) Catalytic mechanism of *S*-adenosylhomocysteine hydrolase. Site-directed mutagenesis of Asp-130, Lys-185, Asp-189, and Asn-190. *J. Biol. Chem.* **277**, 22670–22676.